Journal of Materials Chemistry A

Accepted Manuscript

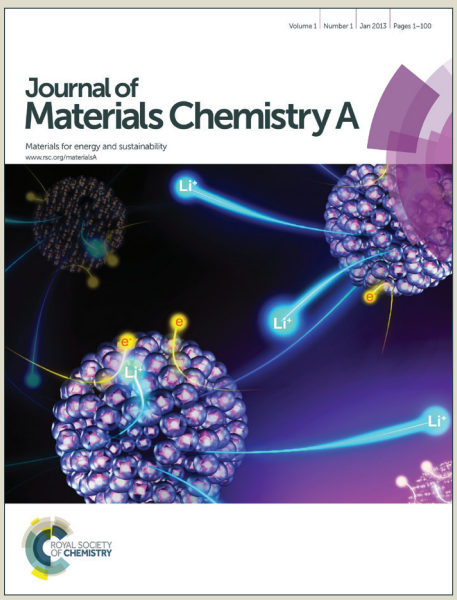

ROYAL SOCIETY OF CHEMISTRY

www.rsc.org/materialsA

Journal of Materials Chemistry A

Dynamic Article Links ►

Cite this: DOI: 10.1039/c0xx00000x

ARTICLE

www.rsc.org/xxxxxx

Self n-Doped [6,6]-Phenyl-C61-butyric Acid 2-((2-(trimethylammonium)ethyl)-(dimethyl)ammonium) ethyl Ester Diiodides as a Cathode Interlayer for Inverted Polymer Solar Cells

Weixiang Jiao,[a †] Di Ma,[bc †] Menglan Lv,[bde] Weiwei Chen,[a] Haiqiao Wang,[c] Jin Zhu,[d] Ming Lei,[a]*and Xiwen Chen[b]*

Received (in XXX, XXX) Xth XXXXXXXXX 20XX, Accepted Xth XXXXXXXXX 20XX
DOI: 10.1039/b000000x

Abstract

A series of self n-doped fullerene ammonium derivatives have been synthesized and confirmed with electron paramagnetic resonance and conductivity measurements. The existence of stable $C_{60}O_2^{\cdot-}$ anion radical in these materials resulted in intrinsically high conductivities between 1.05×10^{-2} and 1.98×10^{-2} S/cm. Among the fullerenes with different number of ammonium and various counter anion, [6,6]-phenyl-C61-butyric acid 2-((2-(trimethylammonium)ethyl)-(dimethyl)ammonium)-ethyl ester diiodides (PCBDANI) showed the best solvent resistance which was confirmed by the measurement of film thickness and corresponding UV-vis absorption before and after rinsed with dichlorobenzene. Most importantly, the inverted polymer solar cells with the structure of ITO/PCBDANI/P3HT:PCBM/MoO_3/Ag remained reasonable high power conversion efficiency even at a thickness of 82 nm of the PCBDANI film as the cathode interlayer. This thickness tolerant cathode interlayer would enable to achieve good device performance with a wider range of film thicknesses and thus large-area device printing this interlayer or on this interlayer could become feasible.

Introduction

Polymer solar cells (PSCs) have attracted broad interests both in academic and industry as renewable energy sources because of their unique advantages of light weight, flexible and low cost fabrication.[1-7] So far, tandem solar cells reached a power conversion efficiency (PCE) of 10.6 %[8] while single junction cells showed the highest PCE of 9.35 %[9] based on an inverted polymer solar cell (I-PSC) with a cathode interfacial layer processed with an alcohol. Cathode interfacial materials are one of the key components for efficient polymer solar cells.[8-50] In recent years, water-soluble or alcohol-soluble polar polymers have been successfully employed as the cathode interlayers in conventional and inverted PSCs including poly(ethylene oxide),[14-17] conjugated polyfluorene derivatives with the side chains containing amino- end groups[18-28] or phosphoryl end groups[29-31] or metal ion-intercalated crown ether,[32] amino-containing insulating polyethylenimine derivatives,[33-35] a hyperbranched conjugated polymer,[36] and conjugated polymeric zwitterions.[37] Moreover, fullerene derivatives and cross-linked fullerenes have been intensively studied due to their electron transport properties.[38-52] The interfacial dipole formation between an amine and a metal electrode, and n-doping of conducting fullerenes are the main reasons for the improvement of device performance.

Usually, semiconducting cathode interlayers were thin in thickness around 5~10 nm in order to achieve optimized device performance because thick interlayer will result in a high series resistance, while a very thin layer could not provide an ohmic contact for electron extraction and transport. However, to print this thin layer or to print on this thin layer is challenging for large area device fabrication.[21,32,53,54] Thus thickness tolerant interlayers which possess excellent electron transport property and solvent resistance would have significant advantages.

Recently, Huang *et al.* reported a mercury-containing alcohol soluble conjugated metallopolymer PFEN-Hg as a cathode interlayer in PSCs with enhanced electron transport property by improving the main chain interaction.[55] Thus PFEN-Hg based device performance exhibited less stringent dependency on the thickness of the interlayer.[55] However, PFEN-Hg is not an environmentally friendly material and will limit its use for large-area device fabrication. More recently, Li *et al.*[56] have demonstrated that perylene diimide derivatives could be used as a thickness-insensitive cathode interlayer for high performance

conventional PSCs in a wide thickness range of 6 to 25 nm.

Electrically doped organic transport layers with high conductivity can facilitate charge carrier transport both in organic light-emitting diodes and organic solar cells.[57] However, an efficient n-type molecular doping is intrinsically more difficult than p-type doping since the HOMO level of the dopant must be higher than the LUMO level of the matrix material, which makes such materials vulnerable to oxidation in ambient. In addition, it is difficult to find suitable dopants with increasing HOMO level. The current n-doping approaches such as thermal evaporation of small molecules and *in situ* creation of volatile dopants from precursors need inert environment and have been hindered by aggregation of small dopants in solid-state.[57-58] Therefore, the development of solution processible and stable n-doped cathode interfacial materials for PSCs device fabrication is of great challenge.

More recently, Jen *et al.* demonstrated a self n-doped fullerene with an ammonium salt (FPI)[59] and further effective doping of fullerenes *via* simple solution-processed blend of [6,6]-phenyl-C61-butyric acid methyl ester (PCBM) and tetrabutylammonium salts[60] to achieve high conductivity in thin films. Lonergan[61] also confirmed the n-doping but proposed a mechanism involving chemical reaction before the electron transfer induced n-doping. However, the feasibility of using FPI as a cathode interlayer for I-PSCs is limited because FPI possesses poor orthogonal solvent processability as it can be dissolved in common organic solvents such as chlorobenzene in which the top layer was formed from its solution.[62] Most interlayers such as poly[(9,9-bis(3´-(N, N-dimethylamino)propyl)-2,7-fluorene)-alt-2,7-(9,9-dioctylfluorene)] (PFN) or fullerene derivatives can be dissolved in common solvents and cross-linking has been used for improving the solvent resistance in organic light emitting diodes[53,63,64] and PSCs.[14,28,42,43,55] Similarly, FPI has to be embedded into a thermally cross-linked semiconducting fullerene matrix.[62] Although doped and solvent resistant interlayer was obtained, it became less conductive by this blending and thus the performance of the solar cells is sensitive to its thickness.[62]

Previously, we reported an alcohol soluble fullerene derivative, [6,6]-phenyl-C61-butyric acid 2-((2-(trimethylammonium)ethyl)(dimethyl)ammonium)-ethyl ester diiodides (PCBDANI) as a cathode interlayer successfully in conventional PSCs.[45] In this paper, we report that a few intrinsically conductive fullerene derivatives with different number of ammonium salts and various counter ions are self n-doped, which is confirmed with electron paramagnetic resonance (ESR) and conductivity measurements. PCBDANI is shown to have the best solvent resistance and thickness tolerance as the cathode interfacial layer in a proof-of-concept I-PSCs with device architecture ITO/interlayer/P3HT:PCBM/MoO_3/Ag where P3HT represents poly(3-hexylthiophene), a typical donor for PSCs. Notably, the devices could remain high efficiency even at a thickness of 82 nm of the PCBDANI film.

Experimental

Materials: All solvents were purchased from Sigma Aldrich, P3HT from Merck Chemicals Ltd and PCBM from Nano-C. Inc.

Synthesis and characterization of PCBANI and PCBDANBr

Similar to PCBDANI,[45] [6,6]-phenyl-C61-butyric acid trimethylaminoethyl ester iodide (PCBANI) and [6,6]-phenyl-C61-butyric acid 2-((2-(dimethylethanammonium)ethyl)(methyl) amino)ethyl ester bromide (PCBDANBr) in Scheme 1 were synthesized using PCBM as the starting material. [6,6]-Phenyl-C61-butyric acid (PCBA) and [6,6]-phenyl-C61-butyric acid chloride (PCBA-Cl) were prepared as before.[45] Esterification of PCBA-Cl with 3-(dimethylamino)propan-1-ol and 2-((2-(dimethylamino)ethyl)(methyl)-amino)ethanol afforded [6,6]-phenyl-C61-butyric acid dimethylaminoethyl ester (PCBAN)[42] and [6,6]-phenyl-C61-butyric acid 2-((2-(dimethylamino)-ethyl)(methyl)amino)ethyl ester (PCBDAN)[45] separately, which were allowed to react with iodomethane and bromoethane to obtain PCBANI and PCBDANBr accordingly following the method for preparation of PCBDANI.[45] The structure of PCBANI and PCBDANBr were characterized by using Av400X NMR (Bruker Co.) and Thermo Scientific Q-Exactive FTMS. Both PCBANI and PCBDANI are soluble in methanol and readily soluble in DMF and DMSO. For PCBDANBr, it can be dissolved in DMSO, and mixed solvents of methanol with other solvents such as chloroform or chlorobenzene.

PCBANI. A solution of PCBAN (0.10 g, 0.10 mmol) and methyl iodide (0.5 mL) in chloroform (10 mL) was stirred at room temperature for 24 h. PCBANI precipitated and the suspension was transferred into a centrifuge bottle, centrifuged, decanted and then re-suspended in methanol, centrifuged, decanted, and treated twice with methanol in the same manner. The residue was dried *in vacuo* at room temperature for 48 h to give a brown solid, PCBANI (0.10 g, yield 90 %). ^{1}H NMR (400 MHz, d_6-DMSO, δ): 1.95-2.07 (m, 2H), 2.54-2.58 (m, 2H), 2.83-2.91 (m, 2H), 3.09-3.21 (m, 15H), 3.67-3.74 (m, 2H), 3.86-3.97 (m, 2H), 4.41-4.48 (m, 2H) 7.43-7.47 (m, 1H), 7.51-7.55 (m, 2H), 7.98 (d, 2H, J = 8.0 Hz). ^{13}C NMR (100 MHz, d_6-DMSO, δ): 22.4, 22.8, 33.8, 52.74, 52.95, 61.5, 63.2, 80.6, 129.0, 132.6, 136.8, 137.3, 138.3, 140.7, 140.9, 142.3, 142.4, 142.5, 143.1, 143.9, 144.0, 144.4, 144.6, 144.72, 144.9, 145.2, 145.3, 145.8, 146.4, 148.4, 149.6, 172.9. MALDI-TOF-MS: calcd for $[C_{77}H_{26}NO_2]^+\cdot I^-$, 996.2, found $[M-I]^+$, 996.0.

PCBDANBr. A solution of PCBDAN (0.20 g, 0.18 mmol) and ethyl bromide (0.5 mL) in chloroform (10 mL) was stirred at room temperature for 48 h. The product was purified by neutral aluminium oxide column chromatography successively using chloroform and methanol as the eluents to give a brown solid, PCBDANBr (0.16 g, yield 78 %). ^{1}H NMR (400 MHz, d_6-DMSO, δ): 1.19 (d, 3H, J = 8.0 Hz), 1.97-2.01 (m, 2H), 2.20 (s, 3H), 2.46-2.47 (m, 6H), 2.58-2.60 (m, 2H), 2.70-2.72(m, 2H), 2.85-2.89 (m, 2H), 2.87-2.98 (m, 6H), 4.06-4.09 (m, 2H), 7.46-7.48 (m, 1H), 7.53-7.57 (m, 2H), 8.01 (d, 2H, J = 8.0 Hz). ^{13}C NMR (100 MHz, d_6-DMSO, δ): 8.4, 22.4, 33.4, 33.6, 42.4, 50.3, 51.2, 52.7, 55.7, 59.6, 62.1, 80.5, 128.8, 128.9, 132.5, 136.7, 137.1, 140.5, 140.6, 140.7, 142.0, 142.1, 142.3, 142.87, 142.91, 143.71, 143.74, 144.2, 144.6, 145.1, 145.6, 146.3, 148.4, 149.7, 172.8. MALDI-TOF-MS: calcd. for $[C_{80}H_{33}N_2O_2]^+\cdot Br^-$, 1053.25, found $[M-Br]^+$, 1053.25.

ESR measurements

Sample solutions were added into ESR test tubes and then bubbled with nitrogen to form films on the tube walls at room temperature or at 100 °C under nitrogen atmosphere. ESR

measurements were performed using an ESRA-300 electron paramagnetic resonance spectrometer (Bruker Co.) at room temperature under nitrogen.

Device fabrication and characterization

SCLC device. Electron-only device structures were used: ITO/fullerene (80 nm)/Al (100 nm). The ITO-coated glass substrates were firstly cleaned *via* a four-step solvent cleaning procedure under sonicating which started from detergent, then deionized water, acetone and isopropanol, each for 10 min. Then the substrates were dried before undertaking a 10 min ultraviolet-ozone treatment. After that the substrates were transferred into a glove box with nitrogen atmosphere. PCBANI and PCBDANI were dissolved in DMF while PCBDANBr was dissolved in a mixture of methanol and chlorobenzene. Then the solutions were spin-coated (1000 rpm, 60 s) onto the pre-cleaned substrates. A silver layer with a thickness of 100 nm was deposited on the fullerene layers.

I-PSCs. ITO substrates were cleaned with a neutral detergent solution, deionized water, acetone and isopropyl alcohol sequentially. Then they were treated with UV/ozone at 30 ^{o}C for 10 min. After that the devices were transferred to a glove-box where the fullerene ammonium layers were spin-coated at 700 rpm for 90 s onto the ITO. P3HT and PCBM were dissolved in dichlorobenzene together in 90 ^{o}C for 1 h. Concentration of both P3HT and PCBM was 15 mg/mL. The solution was filtered before being spin coated (1300 rpm, 60 s) on the interlayer coated substrates. The films were thermally annealed at 150 ^{o}C for 10 min. Then a layer of 10 nm MoO_3 was thermally evaporated onto the active layer at a rate of 0.2 Å/s, followed by a layer of 100 nm silver at 3 Å/s at a pressure below 2×10^{-6} Torr. A mask defined the active area of the solar cell device as 10 mm^2. Current density-voltage (J-V) characteristics of the devices were measured using a Keithley 2410 Source Meter Unit. Solar cell performance was measured under an Air Mass 1.5 Global (AM 1.5 G) Oriel solar simulator fitted with a 1000 W Xe lamp, filtered to give an output of 1000 W/m^2 in a glove-box. The incident photon to current efficiency (EQE or IPCE) was measured under ambient atmosphere at room temperature using a Stanford Research Systems model SR830 DSP lock-in amplifier coupled with a WDG3 monochromator and 500W xenon lamp. The light intensity at each wavelength was calibrated with a standard single-crystal Silicon photovoltaic cell. The absorption was measured by Hitachi U-3010 UV-Vis spectrophotometer. A Dektak 6M stylus profiler (Veeco, Inc.) or an Ambios Technology XP-2 surface profilometer was used to measure the thickness of the films. The ultraviolet photoelectron spectroscopy (UPS) measurements were conducted in ultra-high vacuum (3.0×10-8 Torr) with a Kratos Axis Ultra DLD ultraviolet photoelectron spectrometer equipped with a monochromatic He ultraviolet source He I (hv=21.2 eV). To separate the sample and the secondary edge for the analyzer, a sample bias of –9 V was applied.

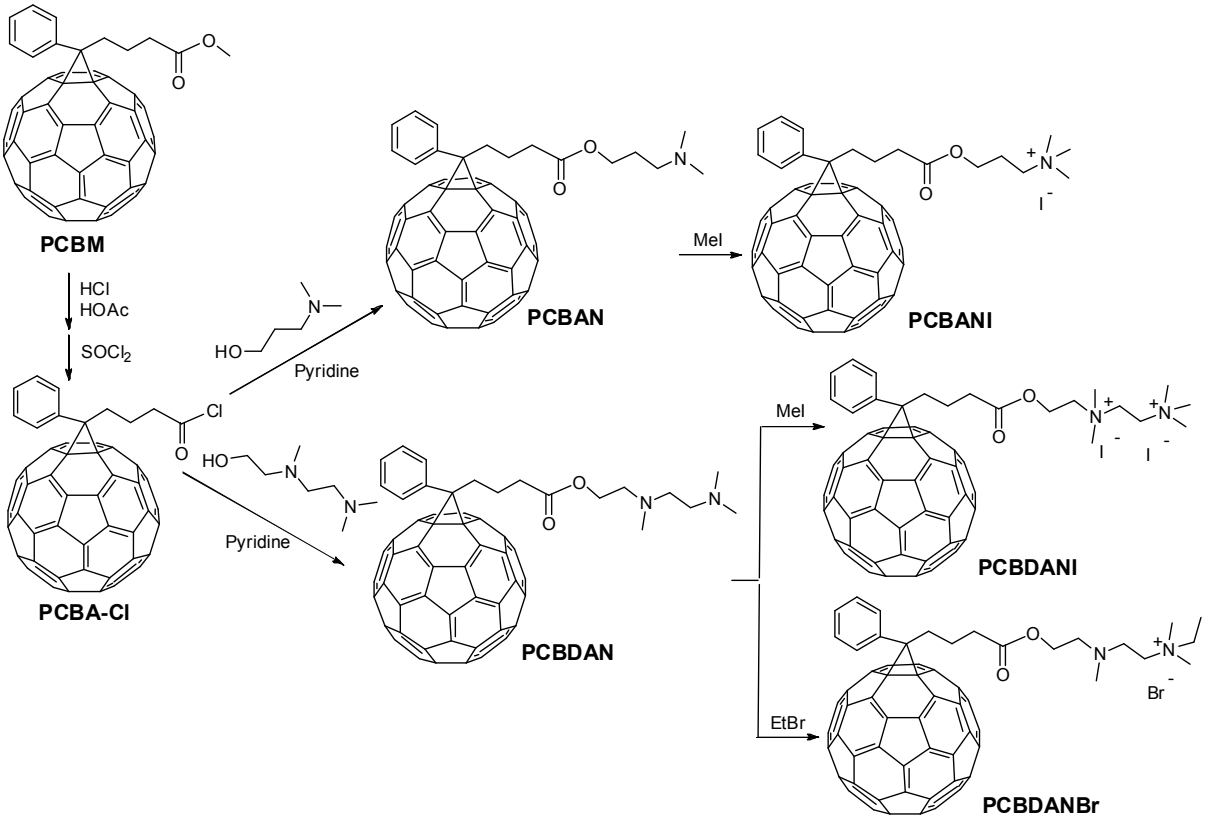

Scheme 1. Synthetic route of PCBDANI, PCBANI and PCBDANBr.

Results and discussion

Journal of Materials Chemistry A

Cite this: DOI: 10.1039/c0xx00000x

www.rsc.org/xxxxxx

ARTICLE

ESR measurements

To confirm the self n-doping of these fullerene derivatives, electron paramagnetic resonance (ESR) were measured. ESR spectra of [6,6]-phenyl-C61-butyric acid trimethylaminoethyl ester iodide (PCBANI), PCBDANI and [6,6]-phenyl-C61-butyric acid 2-((2-(dimethylethanammonium)ethyl)(methyl) amino)ethyl ester bromide (PCBDANBr) films were recorded at room temperature under nitrogen. In Fig. 1a, the paramagnetic signals were observed with g values of 2.0027, 2.0027, and 2.0026 for PCBANI, PCBDANI, and PCBDANBr respectively. In comparison, PCBDAN showed no significant ESR signal, confirming its semiconducting nature. It was reported that g value for PCBM anion radical is 1.998.[58] The same g value for C_{60} was reported by Hwang *et al.*[65] They also observed that upon exposure to molecular oxygen the broad C_{60} band was slowly converted to band b with g = 2.0008 and then further transformed to more stable band c with g = 2.0026. At high temperatures (T > 355 K) and in a polar solvent, the band c can be partially reversibly converted back to the band b. Both bands b (g value of 2.0008) and c (g value of 2.0026) were designated to two isomers of the $C_{60}O_2$ anion radical.[65] Similarly, both bands b and c for PCBDANBr film were observed when the sample was prepared at 100 °C under nitrogen (Fig. 1b). The existence of band c or band b suggested that fullerene radical anions do exist in these materials through self n-doping of the fullerenes.[58-60] We note that FPI also has a similar g-factor of 2.0010,[59] which may indicate that FPI is also in the form of $C_{60}O_2$. We believe that insufficient deoxygenation leads to the formation of the $C_{60}O_2$ anion radical which was readily been observed. Fortunately, these materials are stable under ambient condition for processing and still work well in devices as will be disclosed later.

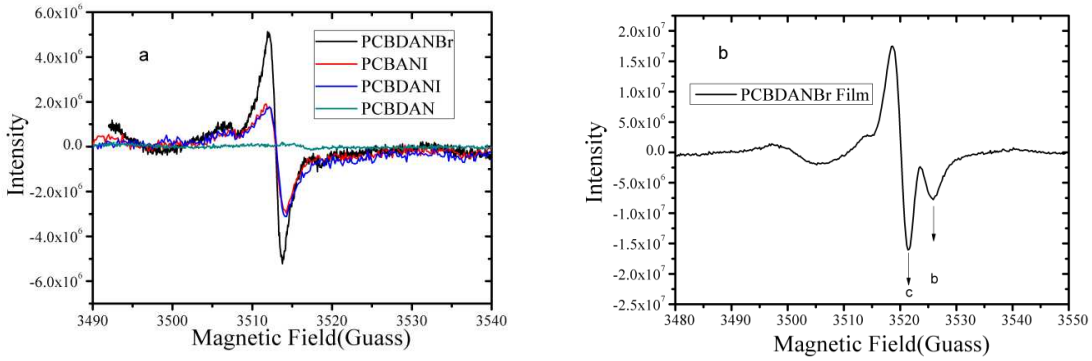

Fig. 1 ESR spectra of PCBANI, PCBDANI, PCBDANBr and PCBDAN films prepared at room temperature (a) and PCBDANBr film prepared at 100 °C under nitrogen (b).

Conductivity measurements

The conductivities of these fullerene ammoniums were tested using space-charge limited current (SCLC) method based on the electron-only devices ITO/fullerene (80 nm)/Al (100 nm). We fitted the experimental J-V data in the logarithmical scales and a slope of 1 instead of 2 was obtained, which indicated there is no SCLC but Ohmic's law was followed (Fig. 2). Thus these fullerenes are not semiconductors but conducting materials, which are in agreement with the ESR measurements. The conductivities for PCBANI, PCBDANI, and PCBDANBr, were 1.50×10^{-2}, 1.98×10^{-2}, and 1.05×10^{-2} S/cm respectively, which are comparable to those for other conducting materials such as FPI (2.0×10^{-2} S/cm),[59] PEDOT-PSS(< ~10^{-3} S/cm for Baytron P VPAI 4083[66] and 0.4 S/cm for Baytron P V4071[67]) and an anionic narrow band gap conjugated polyelectrolyte (1.5×10^{-3} S/cm).[68] The intrinsically high conductivity should be ascribed to the effective n-doping of fullerene films.

Journal of Materials Chemistry A

Dynamic Article Links ►

Cite this: DOI: 10.1039/c0xx00000x

ARTICLE

www.rsc.org/xxxxxx

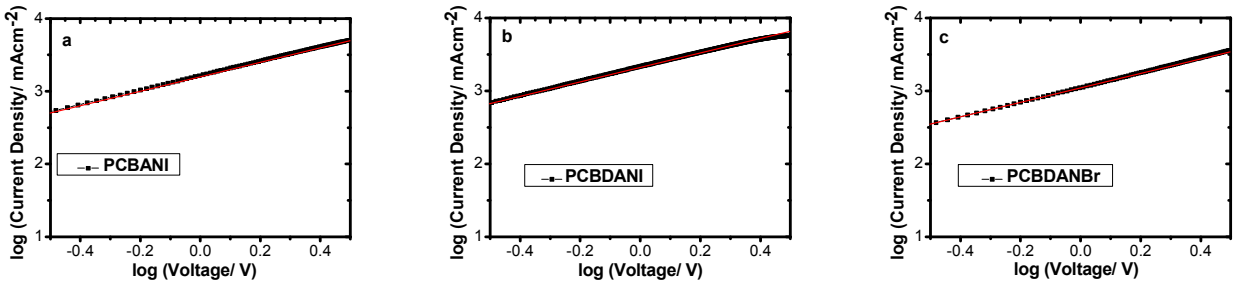

Fig. 2 The current density versus applied voltage (J-V) characteristics of electron-only devices ITO substrate/fullerene/Al. (black line measured and red line fitted from SCLC model): PCBANI (a); PCBDANI (b); PCBDANBr (c).

Solvent resistance test

Solvent resistance of these materials were studied by the measurement of film thickness and corresponding UV-vis absorption before and after rinsed with dichlorobenzene. Spin coating from 40 mg/mL solutions in DMF, PCBDANI and PCBANI films had thickness of 84 and 85.5 nm, respectively. After rinsed with dichlorobenzene, the thickness became 82 and 54.6 nm respectively. For PCBDANBr film, a thickness of 105 nm has been fabricated by multi-layer casting from its methanol solution and it became 63 nm after rinsed with dichlorobenzene. The measured thicknesses variation was in agreement with the UV-vis absorption (Fig. 3). Thus PCBDANI has the best solvent resistance, and the actual thickness (82 nm) was extraordinarily high for the film prepared at 40 mg/mL. The tuning of the solvent resistance property has been achieved with different numbers of ammonium and various counter ions, and further optimization of solvent resistance could be possible by structure modification.

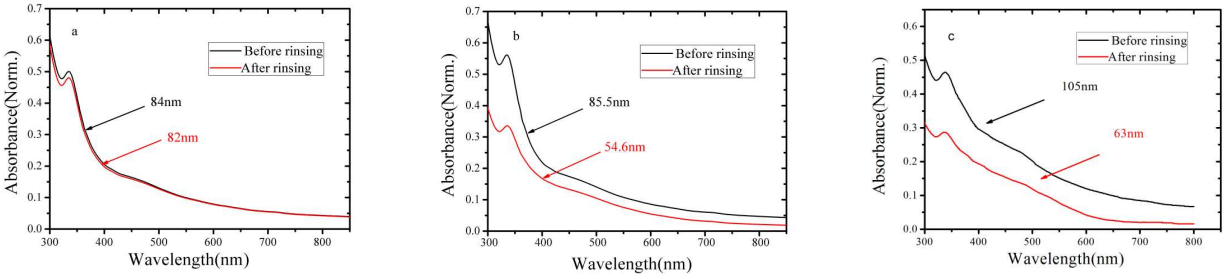

Fig. 3 UV-vis spectra of PCBDANI (a), PCBANI (b) and PCBDANBr (c) films before and after rinsed with dichlorobenzene.

Work function of ITO coated with interlayers

The banding energies of bare ITO and ITO coated with various interlayer films were measured by UPS (**Fig. 4**). Thus the work function of pristine ITO is decreased from 4.67 to 4.27, 4.23 and 4.19 eV for the ITO coated with PCBANI, PCBDANI and PCBDANBr respectively. These results indicate that all of these materials could be used as cathode interlayer in I-PSC.

Photovoltaic devices study

High conductivities of the self n-doped fullerenes suggested that they would be potentially thickness tolerant as cathode interlayers. To prove this concept, the effect of the thickness of the three fullerene interlayers on the I-PSC performance was examined. The device structure for evaluating the material was ITO/interlayer/P3HT:PCBM/MoO_3/Ag, where ITO was used as

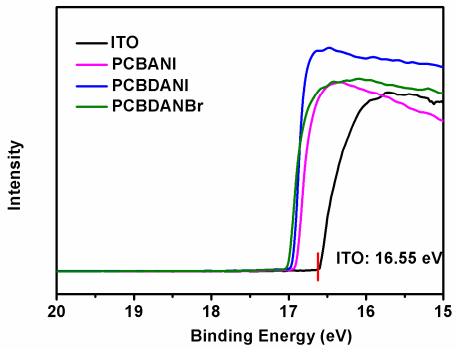

Fig. 4 Ultraviolet photoelectron spectroscopy (UPS) of bare ITO and ITO coated with various interlayer films.

Journal of Materials Chemistry A

Cite this: DOI: 10.1039/c0xx00000x

www.rsc.org/xxxxxx

ARTICLE

the cathode, MoO_3/Ag as the anode, P3HT and PCBM used as the donor and acceptor respectively. A series of PCBDANI and PCBANI films with various thicknesses were spin-coated atop ITO substrates from their DMF solutions while PCBDANBr films were spin cast from the solution in mixture solvent of methanol and chlorobenzene. For comparison, a control device without any interlayers was also fabricated. The current density-voltage (*J-V*) curves for the I-PSCs measured under AM 1.5 G irradiation (1000 W m^{-2}) and dark are presented in Fig. 5 and the corresponding device characteristics including J_{sc}, V_{oc}, *FF* and PCE values are summarized in Table 1. The relationship of PCE *versus* interlayer concentration was plotted in Fig. 6. I-PSC with a bare ITO electrode performed poor with a PCE of 0.32 %, a J_{sc} of 6.96 mA cm^{-2}, a V_{oc} of 0.14 V, and a *FF* of 31.7 %. With a thin interlayer, the devices worked reasonable well for all three interlayers. The optimized devices appeared for all the interlayers cast from low concentrations: V_{oc} reached 0.58 V, J_{sc} reached 10.1~10.2 mA/cm^2, *FF* reached 64.0~66.4 % and PCE reached 3.62~3.83 %. For the interlayers with iodide counter ions, the PCEs remained as high as over 90% of the maximum PCEs when the interlayers were spin cast from 40 mg/mL concentration, the highest concentration test in this work. These performances are comparable to that from inverted solar cells with other cathode interlayers.[47,69-71] While, PCBDANBr gave worse performance at high concentrations, due to solubility issue after the material was stored for a period of time. Notably, for PCBDANI film prepared at 40 mg/mL, the thickness reaches 82 nm. At this extraordinarily high thickness, the device remains PCE as high as 90% of the maximum (3.43 % versus 3.82%) with even higher *FF* (66.4 %), along with the reduced R_s and increased R_{sh}. However, its J_{sc} (9.05 mA/cm^2) was reduced by 10 % relative to the maximum value. To understand why the J_{sc} is reduced, we measured the UV-vis spectra (**Fig. 7**) and external quantum efficiency (EQE, **Fig. 8**.) of the devices with PCBDANI interlayer spin cast from 1, 6 and 40 mg/mL concentration and the control device without PCBDANI interlayer. The average thicknesses of these interlayers are around 5, 23, and 82 nm respectively. Indeed, the interlayer contributed to the absorption at short wavelength peaking at ~330 nm, and extending to long wavelength as seen from both fig. 7 and fig. 3a. From fig. 8, the integrated current is 6.9, 9.8, 10.0, and 8.9 mA/cm^2 for the device at the interlayer thickness of 0, 5, 23 and 82 nm, respectively. These are very close to the measured J_{sc} (Table 1). For thick PCBDANI film of 82 nm, the IPCE is weaker at short wavelength, indicating that the n-doped interlayer absorbed in this region but did not contribute to the photon current, reducing the EQE in this region. In real application, however, this extra-large thickness would be not necessary. The high *FF* along with reduced R_s and increased R_{sh} indicated that the interface between the interlayer and the active layer remained optimized in the case of thick interlayer. In case of PCBANI as the interlayer, J_{sc} decreased only by 2 % relative to the value at its maximal PCE, while the *FF* decreased along with slightly increased R_s. The actual PCBDAN thickness (~55 nm) smaller than PCBDANI of 82 nm could be part of the reason for the various J_{sc}. In addition, while the conductivities of PCBDANI and PCBANI are similar, PCBDANI has an extra ammonium salt which does not involve in the self n-doping. This additional ammonium iodide may negatively dope the PCBM in the active layer through inter-diffusion,[72] and made the n-doped region wider than PCBDANI layer itself, and reduced the absorption of the active layer, resulting in lower J_{sc} but good *FF*. However, more works are needed to clarify this point.

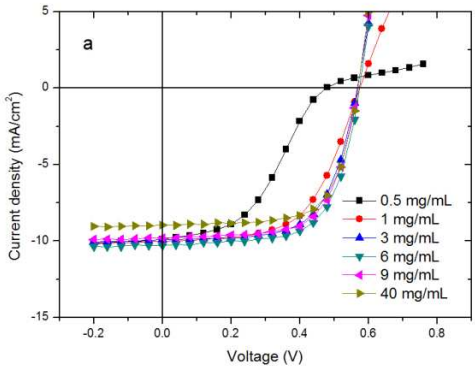

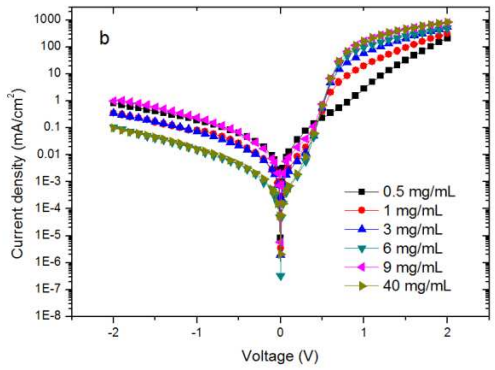

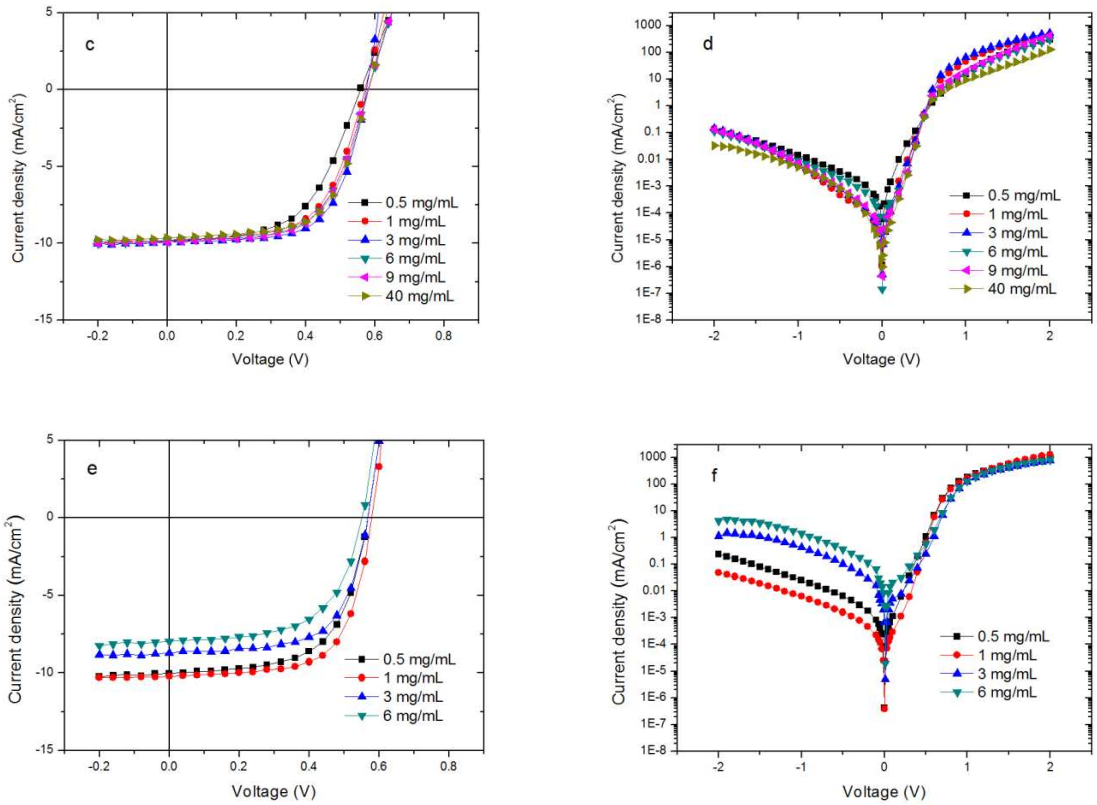

Fig. 5 *J-V* curves of devices ITO/PCBDANI/P3HT:PC61BM/MoO_3/Ag (a, b), ITO/PCBANI/P3HT:PC61BM/MoO_3/Ag (c, d), and ITO/PCBDANBr/P3HT:PC61BM/MoO_3/Ag (e, f) under 1000 W/m^2 at AM 1.5 G illumination and dark.

Table 1 Performance of devices ITO/interlayer/P3HT-PCBM/MoO_3/Ag[a].

interlayer	concentration mg mL^{-1}	V_{oc} V	J_{sc} mA cm^{-2}	FF %	PCE %	R_{sh} kΩ cm^2	R_s Ω cm^2
PCBDANI	0	0.14±0.01	6.96±0.3	31.7±1.4	0.32±0.04	0.03±0.01	5.22±1.4
	0.5	0.47±0.02	9.87±0.21	42.4±1.5	1.97±0.19	6.7±0.6	34.5±5
	1	0.57±0.01	10.1±0.4	56.8±2.9	3.25±0.29	21.7±2.9	11.1±0.9
	3	0.57±0.01	9.75±0.12	64.2±0.7	3.59±0.08	79.6±10.3	5.1±1.1
	6	0.58±0.01	10.1±0.2	65.4±0.5	3.82±0.08	111±7	3.8±0.3
	9	0.57±0.01	9.86±0.14	65.0±2.1	3.66±0.12	136±25	2.0±0.3
	40	0.57	9.05±0.1	66.4±2.5	3.43±0.1	370±53	2.1±0.4
PCBANI	0.5	0.55±0.01	10.1±0.2	54.3±1.8	3.01±0.14	52.6±2.70	5.0±0.2
	1	0.57±0.01	9.88±0.12	58.8±2.9	3.31±0.22	140±15	4.3±0.7
	3	0.57±0.01	9.86±0.11	64.0±1.5	3.62±0.13	425±35	3.0±0.4
	6	0.58±0.01	9.81±0.14	61.1±1.2	3.46±0.09	413±32	11.5±0.1
	9	0.58	9.82±0.12	60.9±0.7	3.47±0.05	734±56	9.3±0.4
	12	0.58±0.01	9.71±0.15	61.5±1.1	3.45±0.08	524±29	11.4±0.7
	15	0.58	9.69±0.2	61.4±1.0	3.45±0.13	660±53	13.6±0.2

	18	0.58	9.68±0.13	61.6±0.8	3.47±0.07	713±28	11.5±0.5
	21	0.58±0.01	9.62±0.11	62.0±0.8	3.46±0.08	708±65	24.1±1.1
	40	0.58	9.65±0.15	61.9±1.4	3.45±0.12	463±38	27.6±2.1
PCBDANBr	0.5	0.56	10.0±0.2	61.4±2.5	3.46±0.16	81.1±10.6	1.80±0.2
	1	0.58	10.2±0.1	65.0±0.6	3.83±0.07	303±44	1.90±0.3
	3	0.57	8.71±0.18	64.5±1.1	3.19±0.04	10.4±0.9	1.7±0.1
	6	0.55	7.83±0.3	60.5±2.4	2.60±0.12	1.99±0.37	1.6±0.1

[a] Average and standard deviation based on six 0.10 cm^2 devices on a single chip.

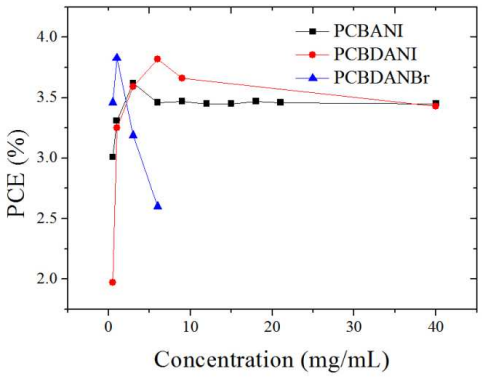

Fig. 6 PCE *versus* concentrations of interlayers in the I-PSCs.

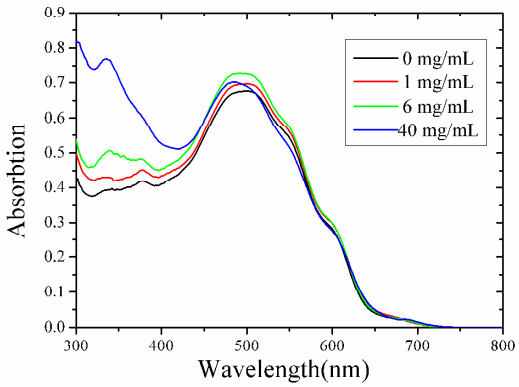

Fig. 7 UV-vis spectra of PCBDANI film spin casted from various concentrations as indicated.

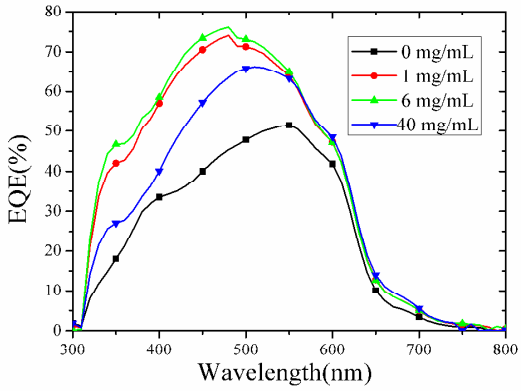

Fig. 8 EQE of I-PSCs devices with various PCBDANI thickness.

Conclusion

Self n-doped fullerene ammonium derivatives: PCBANI, PCBDANI, and PCBDANBr, have been confirmed by ESR, and conductivity measurements. The fullerene anions were in the form of $C_{60}O_2^{\cdot -}$ anion radical as prepared. They are stable under ambient condition for processing and possess high conductivities due to self n-doped nature. Among the interlayers with different numbers of ammonium salts and different counter ions, PCBDANI showed the best solvent resistance to dichlorobenzene and the device PCE remained as high as 3.43 % (versus 3.83% maximum value) at the interlayer thickness of 82 nm. Further optimization of the structure and the processing conditions for this kind of interfacial materials would enable to achieve good device performance with a wider range of film thicknesses and large-area device processing possible. In addition, the self n-doped materials with high conductivity could also be applied in other devices such as perovskite solar cells.[73,74]

Acknowledgements

W. X. Jiao and D. Ma contributed equally to this work. This work was supported by CSIRO through CAS-CSIRO joint project, the Research Program of Educational Bureau of Zhejiang Province of China (No. 20130467).We would like to thank Prof. Jiming Hu at Zhejiang University for his help in some film thickness measurements, Prof. Yongfang Li, Dr. Zhi-Guo Zhang and Xia Guo for their help on the measurements of UPS, EQE and the related UV-vis spectra.

Notes and references

[a]*Department of Chemistry, Zhejiang University, Hangzhou, 310027 P. R. China. Fax: 86 571 87951895; Tel: 86 571 87952359; E-mail: leiming@zju.edu.cn*
[b]*CSIRO Materials Science and Engineering, Clayton, VIC 3168, Australia. Tel: 61 425279534; E-mail: xwchen5702@hotmail.com*
[c]*State Key Laboratory of Organic-Inorganic Composites, Key Laboratory of Carbon Fiber and Functional Polymers, Ministry of Education, Beijing University of Chemical Technology, Beijing, 100029, P. R. China.*
[d]*Chengdu Institute of Organic Chemistry, Chinese Academy of Sciences, Chengdu, 610041, P. R. China.*
[e]University of Chinese Academy of Sciences, Beijing, 100049, P. R. China.

1. G. Yu, J. Gao, J. C. Hummelen, F. Wudl, A. J. Heeger, *Science*, 1995, **270**, 1789.
2. J. Yang, J. You C. C. Chen, W. C. Hsu, H. R. Tan, X. W. Zhang, Z. Hong, Y. Yang, *ACS Nano*, 2011, **5**, 6210.
3. G. Li, R. Zhu, Y. Yang, *Nat. Photon.*, 2012, **6**, 153.
4. Y. F. Li, *Acc. Chem. Res.* 2012, **45**, 723.
5. X. Guo, M. J. Zhang, J. H. Tan , S. Q. Zhang , L.J. Huo, W. P. Hu, Y. F. Li, J. H. Hou, *Adv. Mater.*, 2012, **24**, 6536.
6. M. J. Zhang, Y. Gu, X. Guo, F. Liu, S. Q. Zhang, L. J. Huo, T. P. Russell, J. H. Hou, *Adv. Mater.*, 2013, **25**, 4944.
7. M. J. Zhang, X. Guo, W. Ma, S. Q. Zhang, L. J. Huo, H. Ade, J. H. Hou, *Adv. Mater.*, 2014, **26**, 2089.
8. J. B. You, L. T. Dou, K. Yoshimura, T. Kato, K. Ohya, T. Moriarty, K. Emery, H. C. Chen, J. Gao, G. Li, Y. Yang, *Nat. Commun.*, 2013, **4**, 1446.
9. S.-H. Liao, H.-J. Jhou, Y.-S. Cheng, S.-A. Chen, *Adv. Mater.*, 2013, **25**, 4766.
10. F. Huang, H. B. Wu, Y. Cao, *Chem. Soc. Rev.*, 2010, **39**, 2500.
11. C. H. Duan, K. Zhang, C. M. Zhong, F. Huang, Y. Cao, *Soc. Rev.*, 2013, **42**, 9071.
12. Z. A. Tan, W. Q. Zhang, Y. Huang, Z. G. Zhang, D. P. Qian, J. H. Hou, Y. F. Li, *Adv. Mater.* 2012, **24**, 1476.
13. Z. A. Tan, S. S. Li, F. Z. Wang, D. P. Qian, J. Lin, J. H. Hou, Y. F. Li, *Sci. Rep.*, 2014, **4**, 4691.
14. F. L. Zhang, M. Ceder, O. Inganäs, *Adv. Mater.*, 2007, **19**, 1835.
15. Y. H. Zhou, F. Li, S. Barrau, W. J. Tian, O. Inganäs, F. L. Zhang, *Sol. Energy Mater. Sol. Cells*, 2009, **93**, 497.
16. S. Na, T. Kim, S. Oh, J. Kim, S. Kim, D. Kim, *Appl. Phys. Lett.,* 2010, **97**, 223305.
17. H. L. Yip, A. K.-Y. Jen, *Energy Environ. Sci.*, 2012, **5**, 5994.
18. J. Luo, H. B. Wu, C. He, A. Y. Li, W. Yang, Y. Cao, *Appl. Phys. Lett.* 2009, **95**, 043301.
19. C. He, C. M. Zhong, H. B. Wu, R. Yang, W. Yang, F. Huang, G. C. Bazan, Y. Cao, *J. Mater. Chem.*, 2010, **20**, 2617.
20. L. Zhang, C. He, J. Chen, P. Yuan, L. Huang, C. Zhang, W. Cai, Z. Liu, Y. Cao, *Macromolecules*, 2010, **43**, 9771.
21. Z. He, C. Zhang, X. Xu, L. Zhang, L. Huang, J. W. Chen, H. B. Wu, Y. Cao, *Adv. Mater.*, 2011, **23**, 3086.
22. Z. C. He, C. M. Zhong, X. Huang, W. Wong, H. B. Wu, L. W. Chen, S. J. Su, Y. Cao, *Adv. Mater.*, 2011, **23**, 4636.
23. Y. Dong, X. W. Hu, C. H. Duan, P. Liu, S. J. Liu, L. Y. Lan, D. C. Chen, L. Ying, S. J. Su, X. Gong, F. Huang, Y. Cao, *Adv. Mater.*, 2013, **25**, 3683.
24. Z. C. He, C. M. Zhong, S. J. Su, M. Xu, H. B. Wu, Y. Cao, *Nat. Photon.*, 2012, **6**, 591.
25. T. B. Yang, M. Wang, C. H. Duan, X. W. Hu, L. Huang, J. B. Peng, F. Huang, X. Gong, *Energy Environ. Sci.*, 2012, **5**, 8208.
26. Y. Chen, Z. T. Jiang, M. Gao, S. E. Watkins, P. Lu, H. Q. Wang, X. W. Chen, *Appl. Phys. Lett.*, 2012, **100**, 203304.
27. X. F. Xu, Y. X. Zhu, L. J. Zhang, J. M. Sun, J. Huang, J. W. Chen, Y. Cao, *J. Mater. Chem.*, 2010, **20**, 2617.
28. X. Guo, M. J. Zhang, W. Ma , L. Ye, S. Q. Zhang, S. J. Liu, H. Ade, F. Huang, J. H. Hou, *Adv. Mater.*, 2014, **26**, 4043.
29. Y. X. Zhu, X. F. Xu, L. J. Zhang, J. W. Chen, Y. Cao *Sol. Energy Mater. Sol. Cells*, 2012, **97**, 83.
30. J. M. Sun, Y. X. Zhu, X. F. Xu, L. F. Lan, L. J. Zhang, P. Cai, J. W. Chen, J. B. Peng, Y. Cao, *J. Phys. Chem. C* 2012, **116**, 14188.
31. Y. Zhao, Z. Y. Xie, C. J. Qin, Y. Qu, Y. H. Geng, L. X. Wang, *Sol. Energy Mater. Sol. Cells*, 2009, **93**, 604.
32. S. H. Liao, Y. L. Li, T. H. Jen, Y. S. Cheng, S. A. Chen, *J. Am. Chem. Soc.* 2012, **134**, 14271.
33. Y. H. Zhou, C. Fuentes-Hernandez, J. Shim, J. Meyer, A. J. Giordano, H. Li, P. Winget, T. Papadopoulos, H. Cheun, J. Kim, M. Fenoll, A. Dindar, W. Haske, E. Najafabadi, T. M. Khan, H. Sojoudi, S. Barlow, S. Graham, J. Brédas, S. R. Marder, A. Kahn, B. A. Kippelen, *Science*, 2012, **336**, 327.
34. Y. H. Zhou, C. Fuentes-Hernandez, J. Shim, T. M. Khan, B. Kippelen, *Energy Environ. Sci.*, 2012, **5**, 9827.
35. H. Kang, S. Hong, J. Lee, K. Lee, *Adv. Mater.*, 2012, **24**, 3005.
36. M. L. Lv, S. S. Li, J. J. Jasieniak, J. H. Hou, J. Zhu, Z. A. Tan, S. E. Watkins, Y. F. Li, X. W. Chen, *Adv. Mater.*, 2013, **25**, 6889.
37. F. Liu, Z. A. Page, V. V. Duzhko, T. P. Russell, T. Emrick, *Adv. Mater.*, 2013, **25**, 6868.
38. Q. S. Wei, T. Nishizawa, K. Tajima, K. Hashimoto, *Adv. Mater.*, 2008, **20**, 2211.
39. A. Tada, Y. F. Geng, Q. S. Wei, K. Hashimoto, K. Tajima, *Nat. Mater.*, 2011, **10**, 450.
40. J. W. Jung, J. W. Jo, W. H. Jo, *Adv. Mater.*, 2011, **23**, 1782.
41. K. M. O'Malley, C. Z. Li, H. L.Yip, A. K.-Y. Jen, *Adv. Energy Mater*. 2012, **2**, 82.
42. C. Z. Li, C. C. Chueh, H. L. Yip, K. M. O'Malley, W. C. Chen, A. K.-Y. Jen, *J. Mater. Chem.* 2012, **22**, 8574.
43. C. H. Duan, C. M. Zhong, C. C. Liu, F. Huang, Y. Cao, *Chem. Mater.*, 2012, **24**, 1682.
44. S. S. Li, M. Lei, M. L. Lv, S. E. Watkins, Z. A. Tan, J. Zhu, J. H. Hou, X. W. Chen, Y. F. Li, *Adv. Energy Mater.*, 2013, **23**, 1569.
45. Z.-G. Zhang, H. Li, B. Y. Qi, Z. W. Jin, Z. Qi, D. Chi, J. H. Hou, Y. F. Li, J. Z. Wang, *J. Mater. Chem. A*, 2013, 1, 9624.
46. M. L. Lv, M. Lei, T. Hirai, J. Zhu, X. W. Chen, *ACS Appl. Mater. Interfaces*, 2014, **6**, 5844.
47. D. Hong, M. L. Lv, M. Lei, Y. Chen, P. Lu, Y. G. Wang, J. Zhu, H. Q. Wang, M. Gao, S. E. Watkins, X. W. Chen, *ACS Appl. Mater. Interfaces*, 2013, **5**, 10995.
48. D. Ma, M. L. Lv, M. Lei, J. Zhu, H. Q. Wang, X. W. Chen, *ACS Nano*, 2014, **8**,1601.
49. C. Z. Li, H. L. Yip, A. K.-Y. Jen, *J. Mater. Chem.*, 2012, **22**, 4161.
50. Y. J. Cheng, F. Y. Cao, W. C. Lin, C. H. Chen, C. H. Hsieh, *Chem. Mater.*, 2011, **23**, 1512.
51. C.-Y. Chang, C.-E. Wu, S.-Y. Chen, C. H. Cui, Y.-J. Cheng, C.-S. Hsu, Y.-L. Wang, Y. F. Li, *Angew. Chem. Int. Ed.*, 2011, **50**, 9386.
52. Y.-J. Cheng, C.-H. Hsieh, Y. J. He, C.-S. Hsu, Y. F. Li, *J. Am. Chem. Soc.*, 2010, **132**, 17381.
53. Z. Hua, Y. Zheng, N. L. Liu, N. Ai, Q. Wang, S. Wu, J. H. Zhou, D. G. Hu, S. F. Yu, S. H. Han, W. Xu, C. Luo, Y. H. Meng, Z. X. Jiang, Y. W. Chen, D. Y. Li, F. Huang, J. Wang, J. B. Peng Y. Cao, *Nat. Commun.*, 2013, **4**, 1971.
54. F. C. Krebs, *Sol. Energy Mater. Sol. Cells*, 2009, **93**, 465.
55. S. J. Liu, K. Zhang, J. M. Lu, J. Zhang, H. L. Yip, F. Huang, Y. Cao, *J. Am. Chem. Soc.*, 2013, **135**, 15326.
56. Z. G. Zhang, B. Y. Qi, Z. W. Jin, D. Chi, Z. Qi. Y. F. Li, J. Z. Wang, *Energy Environ. Sci.*, 2014, **7**, 1966.
57. K. Walzer, B. Maennig, M. Pfeiffer, K. Leo, *Chem. Rev.*, 2007, **107**, 1233.
58. B. D. Naab, S. Guo, S. Olthof, E. G. B. Evans, P. Wei, G. L. Millhauser, A. Kahn, S. Barlow, S. R.; Marder, Z. N. Bao, *J. Am. Chem. Soc.*, 2013, **135**, 15018.
59. C. Z. Li, C. C. Chueh, H. L. Yip, F. Z. Ding, X. S. Li, A. K.-Y. Jen, *Adv. Mater.*, 2013, **25**, 2457.
60. C. Z. Li, C. C. Chueh, F. Z. Ding, H. L. Yip, P. W. Liang, X. S. Li, A. K.-Y. Jen, *Adv. Mater.*, 2013, **25**, 4425.
61. C. D. Weber, C. Bradley, M. C. Lonergan, *J. Mater. Chem. A*, 2014, **2**, 303.
62. N. Cho, C. Z. Li, H. L. Yip, A. K.-Y. Jen, *Energy Environ. Sci.*, 2014, **7**, 638.
63. C. M. Zhong, S. J. Liu, F. Huang, H. B. Wu, Y. Cao, *Chem. Mater.*, 2011, **23**, 4870.
64. S. J. Liu, C. M. Zhong, J. Zhang, C. H. Duan, X. H. Wang, F. Hang, *Sci. China Chem.*, 2011, **54**, 1745.
65. Y. L. Hwang, C. C. Yang, K. C. Hwang, *J. Phys. Chem. A*, 1997, **101**, 7971.
66. S. -I. Na, S. -S. Kim, J. Jo., D.-Y. Kim, *Adv. Mater.*, 2008, **20**, 4061.
67. J. Ouang, C. W. Chu, F. C. Chen, Q. Xu, Y. Yang, *Adv. Funct. Mater.*, 2005, **15**, 203.
68. H. Zhou, Y. Zhang, C. K. Mai, S. D. Collins, T. Q. Nguyeb, G. C. Bazan, A. J. Heeger, *Adv. Mater.*, 2014, **26**, 780.
69. B. J. Worfolk, T. C. Hauger, K. D. Harris, D. A. Rider, J. A. M. Fordyce, S. Beaupré, M. Leclerc, J. M. Buriak, *Adv. Energy Mater.*, 2012, **2**, 361.
70. K. Sun, B. M. Zhao, A. Kumar, K. Y. Zeng, J. Y. Ouyang, *ACS Appl. Mater. Interfaces*, 2012, **4**, 2009.

71. V. Murugesan, K. Sun, J. Y. Ouyang, *Appl. Phys. Lett.*, 2013, **102**, 83302.
72. N. D. Treat, M. A. Brady, G. Smith, M. F. Toney, E. J. Kramer, C. J. Hawker, M. L. Chabinyc, *Adv. Energy Mater.*, 2011, **1**, 82.
73. O. Malinkiewicz, A. Yella, Y. H. Lee, M. Espallargas, M. Graetzel, M. K. Nazeeruddin, H. J. Bolink, *Nat. Photon.*, 2014, **8**, 128.
74. D. Liu, T. L. Kelly, *Nat. Photon.*, 2014, **8**, 133.

For Table of Content

Among alcohol soluble self n-doped fullerene ammonium derivatives, the title fullerene showed the best solvent resistance and inverted polymer solar cells remained high efficiency at 82 nm of this interlayer.

Keyword polymer solar cells, n-doped fullerene, cathode interfacial layer, ammonium-modified fullerene

Weixiang Jiao,[a †] Di Ma,[bc †] Menglan Lv,[bdg] Weiwei Chen,[a] Haiqiao Wang,[c] Jin Zhu,[d] Yongfang Li,[ef] Ming Lei,[a]* and Xiwen Chen[b]*

Self n-Doped [6,6]-Phenyl-C61-butyric Acid 2-((2-(trimethylammonium)ethyl)-(dimethyl)ammonium) ethyl Ester Diiodides as a Cathode Interlayer for Inverted Polymer Solar Cells